Received: 16 September 2022 | Revised: 24 May 2023 | Accepted: 13 June 2023

DOI: 10.1111/jsr.13981

RESEARCH ARTICLE

Interrelations and functional roles of key oscillatory activities during daytime sleep in older adults

Larissa N. Wüst[1,2,3] | Daria Antonenko[1] | Robert Malinowski[1] | Liliia Khakimova[1] | Ulrike Grittner[4,5] | Klaus Obermayer[6] | Julia Ladenbauer[1] | Agnes Flöel[1,7]

[1]Department of Neurology, Universitätsmedizin Greifswald, Greifswald, Germany

[2]Centre for Chronobiology, Psychiatric Hospital of the University of Basel, Basel, Switzerland

[3]Research Platform Molecular and Cognitive Neurosciences, University of Basel, Basel, Switzerland

[4]Berlin Institute of Health, Berlin, Germany

[5]Institute of Biometry and Clinical Epidemiology, Charité – Universitätsmedizin, Berlin, Germany

[6]Fakultät IV and Bernstein Center for Computational Neuroscience, Technische Universität Berlin, Berlin, Germany

[7]German Centre for Neurodegenerative Diseases (DZNE) Greifswald, Greifswald, Germany

Correspondence
Julia Ladenbauer, University Medicine Greifswald, Ferdinand-Sauerbruch-Straße, 17475 Greifswald, Germany,
Email: julia.ladenbauer@med.uni-greifswald.de

Agnes Flöel, University Medicine Greifswald, Ferdinand-Sauerbruch-Straße, 17475 Greifswald, Germany.
Email: agnes.floeel@med.uni-greifswald.de

Funding information
Deutsche Forschungsgemeinschaft, Grant/Award Numbers: 327654276 - SFB 1315 B03, to AF and KO

Summary

Certain neurophysiological characteristics of sleep, in particular slow oscillations (SOs), sleep spindles, and their temporal coupling, have been well characterised and associated with human memory abilities. Delta waves, which are somewhat higher in frequency and lower in amplitude compared to SOs, and their interaction with spindles have only recently been found to play a critical role in memory processing of rodents, through a competitive interaction between SO–spindle and delta–spindle coupling. However, human studies that comprehensively address delta wave interactions with spindles and SOs, as well as their functional role for memory are still lacking. Electroencephalographic data were acquired across three naps of 33 healthy older human participants (17 female) to investigate delta–spindle coupling and the interplay between delta- and SO-related activity. Additionally, we determined intra-individual stability of coupling measures and their potential link to the ability to form novel memories in a verbal memory task. Our results revealed weaker delta–spindle compared to SO–spindle coupling. Contrary to our initial hypothesis, we found no evidence for an opposing dependency between SO- and delta-related activities during non-rapid eye movement sleep. Moreover, the ratio between SO- and delta-nested spindles rather than SO–spindle and delta–spindle coupling measures by themselves predicted the ability to form novel memories best. In conclusion, our results do not confirm previous findings in rodents on competitive interactions between delta activity and SO–spindle coupling *in older adults*. However, they support the hypothesis that SO, delta wave, and spindle activity should be jointly considered when aiming to link sleep physiology and memory formation.

KEYWORDS
phase–amplitude coupling, slow oscillation/delta nesting index

Julia Ladenbauer and Agnes Flöel shared-last authorship.

1 | INTRODUCTION

Specific brain oscillations during human non-rapid eye movement (NREM) sleep, most importantly thalamo-cortical spindles (12–15 Hz) and cortical slow-wave activity (SWA), which can be divided into slow oscillations (SOs, 0.5–1 Hz) and delta waves (1–4 Hz) (Steriade, Nunez, Amzica, 1993), have been linked to successful memory consolidation, and thus, the ability to retain novel memories (Rasch & Born, 2013). The differentiation between SOs and delta waves can be made based on their origin, frequency, extent, and amplitude (Genzel et al., 2014; Steriade, Nunez, Amzica, 1993). SOs are generated within cortical networks and exhibit high-amplitude oscillations with a frequency of <1 Hz. Delta waves, by contrast, result from the interaction between pace-making thalamic neurons and the neocortex and are higher in frequency (1–4 Hz) and lower in amplitude.

In humans, the role of SOs for memory processes has been extensively investigated. As such, previous studies have shown increased SO activity after learning, correlating with retention performance after sleep (Mölle et al., 2009). There is also growing evidence that temporal co-ordination of SOs with spindles, rather than SO activity in isolation, is crucial for memory consolidation (Helfrich et al., 2018; Ladenbauer et al., 2017). Moreover, SO–spindle coupling was shown to substantially vary between individuals, but to be stable intra-individually, indicating that this parameter may be a general trait (Cox et al., 2018). This observation may have implications for individual memory abilities beyond sleep-related memory consolidation, namely the ability to form novel memories. With regard to delta waves most studies have considered SO and delta activity jointly as SWA, thus precluding investigation of delta-coupling behaviour with spindles, as well as any attempt to delineate their distinct contribution to memory processes (Ngo & Born, 2019).

One recent rodent study suggested a causal role for delta waves and their interaction with spindles for memory (Kim et al., 2019). In this study, disturbance during delta wave up-states by means of optogenetic stimulation led to a relative increase in SO-nested spindles, enhanced re-activation strength in involved neuronal ensembles, and improved memory performance after sleep. Disturbance during SOs had the opposite effect, resulting in a relatively higher number of spindles nested to delta waves, reduced ensemble re-activations, and impaired performance, suggesting the following: first, there seems to be an opposing dependency between SO- and delta wave-generating systems; second, SO and delta waves may have competitive functional roles in memory (Ngo & Born, 2019). While SO-related spindles support memory consolidation, delta-related spindles seem to benefit forgetting, possibly to support downscaling processes during sleep to restore the brain's capacity to learn (Kim et al., 2019). Interestingly, in rats not SO–spindle coupling by itself, but the ratio between SO-nested spindles to delta-nested spindles was the sleep parameter most predictive for memory performance gains after sleep, underscoring their opposing functional roles for memory. Whether these interrelationships also exist in humans is largely unknown but may be particularly valuable when evaluating interventions that are aimed to modulate memory abilities in healthy and pathological ageing.

In the present study, we therefore first aimed to characterise delta–spindle coupling in healthy older adults (aged ≥50 years), and to compare it to SO–spindle coupling. Second, we aimed to address the previously described competitive interplay between SO- and delta-related activities in natural human nap sleep. Third, we investigated stability of SO–spindle and delta–spindle coupling measures over multiple nap sleep assessments to reveal whether these sleep parameters exhibit a trait-like character. Finally, we tested for associations between ability to form novel memories and SO–spindle and delta–spindle coupling measures in healthy older participants.

2 | METHODS

2.1 | Participants and experimental procedure

A total of 33 healthy older adults (17 female; mean [SD, range] age 65.2 [8.3, 50–77] years) were included in the study. Exclusion criteria included history of severe untreated medical, neurological, and psychiatric diseases; subjective cognitive decline; sleep disorders; cognitive impairment; intake of medication acting primarily on the central nervous system; alcohol or substance abuse. Our choice to investigate healthy older individuals was based on the motivation of understanding and eventually improving sleep physiology and memory in ageing. Data were collected within the scope of an extensive study involving several sets of slow oscillatory transcranial direct current stimulation protocols, in addition to the sessions without stimulation that were used in this report (nine sleep sessions in total; three sleep sessions 'without STIM': T1, T2, T3) (Figure 1a). Whereas T1 was always followed by T2 nap session, T3 was one of the seven following sessions (randomised order; please see [Ladenbauer et al., 2022] for more details, ClinicalTrials.gov Identifier: NCT04714879). The three naps were separated by ~5–6 weeks (mean [SD] time between T1 and T2: 31.2 [41.1] days; mean [SD] time between T2 and T3: 45.2 [32.1] days). A comprehensive neuropsychological testing was administered for assessment of cognitive status in each participant (Ladenbauer et al., 2016). Here, we used the Auditory Verbal Learning Test to probe memory performance (see below), which was acquired prior sleep on T1. In each session, participants arrived at the laboratory between 11:30 a.m. and 2:00 p.m. (at a time suiting their daily routine to allow them to sleep). After preparation of polysomnographic recordings, participants were given the opportunity to sleep for a maximum of 90 min. During the naps an electroencephalogram (EEG) was recorded. The study was approved by the local Ethics Committee (Universitätsmedizin Greifswald) and conducted in accordance with the Declaration of Helsinki. Participants gave written informed consent prior to participation.

2.2 | Memory assessment

As part of the neuropsychological assessment, the German version of the Auditory Verbal Learning Test (AVLT) was performed by all

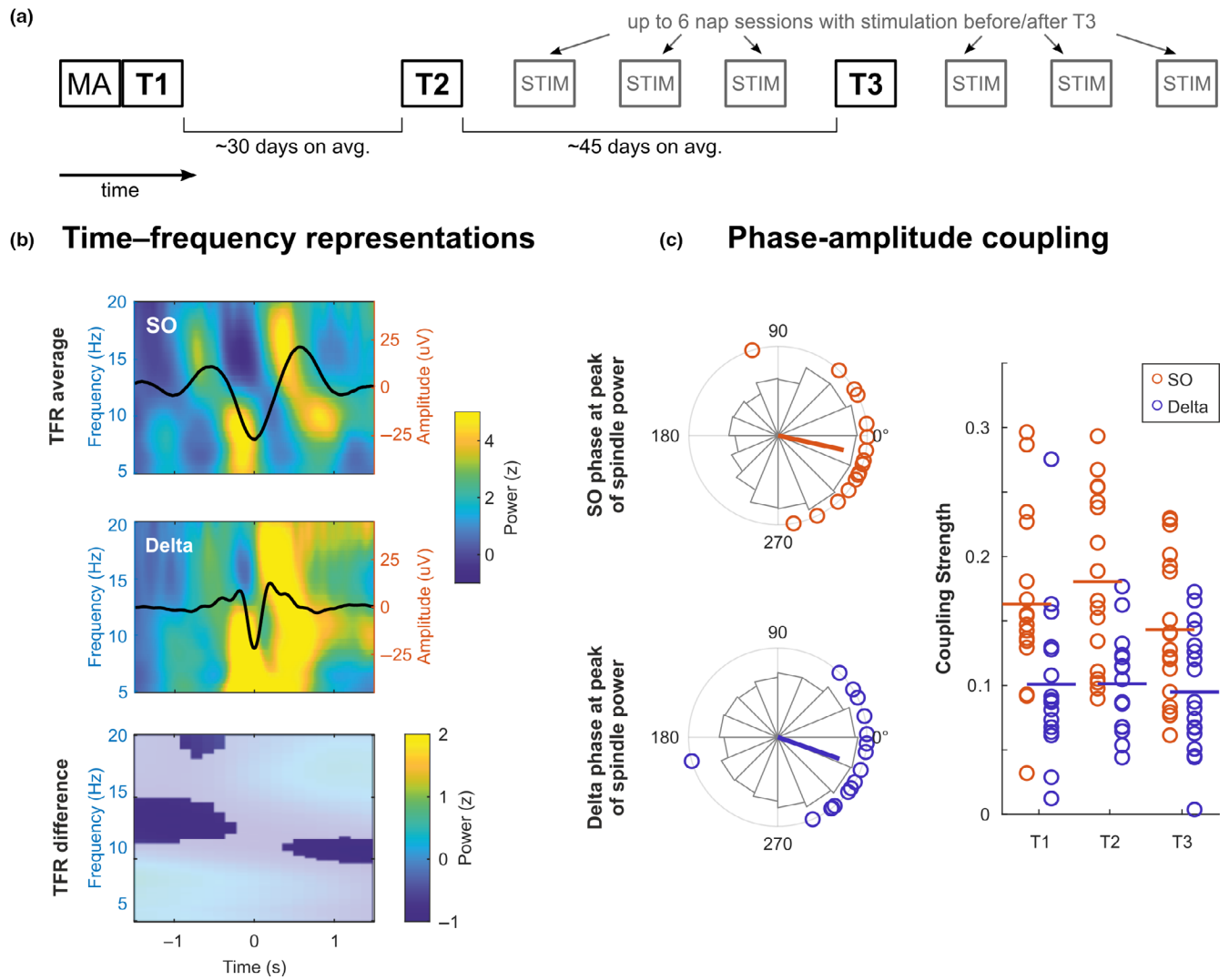

FIGURE 1 (a) Overview of the study procedures, including the six nap sessions with sets of transcranial direct current stimulation (STIM) and the three nap sessions without stimulation, which were employed for the present research question (T1, T2, T3). Whereas T1 was always followed by T2 nap session, T3 was one of the seven subsequent nap sessions that included six nap sessions during which a stimulation was applied, and one nap session with only sham stimulation (T3) (randomised order; please see Ladenbauer et al. (2022) for more details). Memory assessment (MA) of the Auditory Verbal Learning Test took place in the morning before T1. (b) Average time-frequency representations (TFRs) locked to the slow oscillation (SO) trough or delta trough (time 0), respectively. Shown are averaged power z-scores relative to pre-event baseline distributions for the T1 nap session. Black lines indicate grand average electroencephalogram signal of all SO (top, $n = 175$) or delta events (centre, $n = 1091$) aligned to the trough (time 0). Bottom, difference of these TFRs (SO-delta) masked by significance ($p < 0.05$, corrected for multiple comparison). (c) Histogram indicates distribution of SO phase or delta phase angle at peak of spindle power across all SO or delta events, respectively (left). Circles depict individual participants' mean SO phase where spindle power peaks and the coloured line denotes the corresponding resulting vector length across all participants. C: coupling strength (resultant vector length) for SO–spindle (orange) and delta–spindle coupling (blue) per participant (right). Circles depict individual participants and bars the mean coupling strength across participants for each nap condition (T1, T2, T3).

participants to probe memory performance (Helmstaedter et al., 2001). Participants had to learn a list of 15 unrelated words within five immediate auditory presentations, each followed by an attempted recall (termed 'encoding trials'). Subsequently, a second 15-word interference list was presented, followed by retrieval of the initial list. Delayed recall and reScognition were also tested after 30 min. Ability to form novel memories for each participant was indexed by the sum of recalled words from all five encoding trials (encoding performance) as well as by the difference between last encoding and first recall trial after interference (immediate recall performance) (Göder et al., 2013; Mikutta et al., 2019).

2.3 | Electroencephalogram recordings

Polysomnographic data were recorded with a 32-channel Brain Products actiCAP electrode system positioned according to the 10–20 EEG system (reference: nose, ground: FCz) using the BrainAmp DC

amplifier (Brain Products GmbH, Munich, Germany) with a sampling rate of 500 Hz. Horizontal and vertical electro-oculogram (using two electrodes in T1/T2, and four electrodes in T3) and the electromyogram (positioned at the chin) were recorded. Impedances were kept <10 kΩ.

2.4 | Electroencephalogram data analysis

The EEG data were analysed using BrainVision Analyser 2.1 (Brain Products GmbH) and Matlab R2019b (The MathWorks, Inc.) with functions from the FieldTrip (Oostenveld et al., 2011) and CircStat toolboxes (Berens, 2009), as well as custom functions. Prior to sleep scoring and further analysis, data were band-pass filtered (infinite impulse response filter, 0.032–35 Hz, notch: 50 Hz). To eliminate arousal and ocular artefacts, a semi-automatic detection procedure was applied including visual inspection of raw data and an ocular correction procedure by means of independent component analysis. Sleep stages were scored based on standard criteria (Rechtschaffen & Kales, 1968), as EEG derivations recommended by the American Academy of Sleep Medicine (AASM) were occupied by stimulation electrodes in one of three naps. Sleep Stages 3 and 4 were summarised as N3 in the subsequent analyses according to the AASM guidelines. Only naps with a minimum duration of N2/N3 of 15 min were included in the analysis, resulting in the following number of excluded naps: four in T1, four in T2, and one in T3, with a maximum of one excluded nap per participant. Thus, nine (27%) participants were included in the analysis with only two naps instead of three. To characterise the temporal relationship between SOs and spindles, as well as delta waves and spindles, we performed time–frequency representations (TFRs) and phase–amplitude coupling (PAC) analysis for frontal (Fz, FC1, FC2) and centro-parietal (Cz, CP1, CP2) regions of interest (ROIs) (Ladenbauer et al., 2017). These were calculated on 30-s non-overlapping epochs of N2 and N3 (sampling rate 500 Hz). The ROIs were selected on the basis of previous research indicating fronto-central and parieto-central dominance of SOs and spindles, as well as their coupling (Helfrich et al., 2018; Mölle et al., 2011). Given the well-described more local and frontal topographical prominence of delta waves (Bernardi et al., 2018), these ROIs are likewise suitable for delta–spindle coupling.

2.4.1 | Slow oscillation, delta wave, and spindle detection

The SOs of interest were detected using procedures previously applied in several studies (Helfrich et al., 2018; Ladenbauer et al., 2021; Mölle et al., 2002; Staresina et al., 2015). Only artefact-free data from N2 and N3 were used for event detection. For SO event detection, EEG-data were band-pass filtered at 0.16–1.25 Hz (two-pass finite impulse response [FIR] band-pass filter, order = three cycles of the low cut-off frequency). All downward zero crossings were marked as potential start- and end-points of discrete SO oscillations. The time between two successive downward zero crossings was determined, and events were considered SOs for durations between 1 and 2 s, corresponding to a frequency of 0.5–1.0 Hz. For all selected events, the trough-to-peak amplitude was determined. The 25% of events with the largest amplitudes were considered SOs and included in further analysis. For delta-wave detection, EEG-data was band-pass filtered at 0.75–4.25 Hz (two-pass FIR band-pass filter, order = three cycles of the low cut-off frequency). Time between successive downward zero crossings needed to be 0.25–1 s, corresponding to a frequency of 1–4 Hz for an event to be considered a delta wave. Only the 25% of events with the highest amplitudes were considered delta waves and included in further analysis. For spindle detection, we similarly used procedures that were applied in previous studies (Helfrich et al., 2018; Ladenbauer et al., 2021; Mölle et al., 2009). First, EEG-data was band-pass filtered at 12–15 Hz (two-pass FIR band-pass filter, order = three cycles of the low cut-off frequency). Root mean square (RMS) values of the filtered signal were calculated with a moving average of 200 ms. Events with RMS amplitude values above an individual threshold determined as the 25% of spindle events with the highest RMS amplitude values for a duration of 0.5–3 s were considered spindle events. Artefact-free segments of ±2.5 s around the event centres (SO/delta wave trough or spindle centre) were extracted from the unfiltered signal for further analysis. To address the issue of spurious cross-frequency coupling, which can be caused by differences in oscillatory power (Aru et al., 2015), we performed a normalisation of individual events to minimise amplitude differences prior to all subsequent analyses.

2.4.2 | Temporal relationships of SOs, delta waves, and spindles

The present investigation builds on the compelling evidence for the distinction between SOs and delta waves (Achermann & Borbély, 1997; Mölle et al., 2002; Steriade, McCormick, D. & Sejnowski, 1993), and primarily addresses the competitive interplay between SO- and delta-related activities, previously described only in rodents, and their functional roles in memory in older humans. We used several complementary approaches to investigate the temporal relationships between SOs, delta waves, and spindles: TFR analyses, PAC analyses, and — in accordance with the rodent study (Kim et al., 2019) — an analysis on the ratio between SO-related spindles to delta-related spindles (SO/delta nesting index) that was most informative for memory performance in rodents. For this purpose, discrete spindles were detected that occurred in temporal proximity to SOs or delta waves (please see below for more details). To address the suggested interdependence between SO- and delta-related activities, we also compared SO–spindle coupling in low–high delta power segments.

Time–frequency representation. For the TFR analyses, detected SO and delta event segments were normalised using a z-score based on the mean and standard deviation calculated from the averaged event segment per participant and channel as established in previous studies

(Ladenbauer et al., 2021). TFRs were calculated to display spectral densities of frequencies between 5 and 20 Hz in a time window of ±1.25 s around the SO trough. Therefore, spectral densities were calculated in 0.25-Hz steps using a sliding (10-ms steps) Hanning tapered window with a variable, frequency-dependent length. The window length always comprised a full number of five cycles to ensure reliable power estimates. The baseline interval (−2.5 to −1.25 s) was used for a baseline correction of TFRs. The TFRs were then averaged across all segments and all electrodes of the respective ROI for each nap. The same procedure was applied to the delta event segments.

Phase–amplitude coupling. In addition, we determined PCA between SOs and spindle activity based on previous studies (Helfrich et al., 2018; Ladenbauer et al., 2021), which allows a more precise characterisation of coupling independent of their frequency. Thereby two parameters for each participant and nap were obtained: the SO phase of peak spindle power and the resultant vector length that represents the coupling strength between the two oscillations. We therefore filtered the normalised SO event segments in the SO frequency band (0.16–1.25 Hz) and extracted the instantaneous phase angle using the Hilbert transform. Subsequently, the same segments were filtered in the spindle frequency band (12–15 Hz) and the instantaneous amplitude was extracted from the Hilbert transform. We only considered the time range −2 to +2 s to avoid filter edge artefacts. In a next step, the maximum spindle amplitude and corresponding SO phase was extracted for each participant, nap, channel, and SO event. Finally, we determined the mean SO phase and corresponding resultant vector length across all events for each participant and nap using the CircStat toolbox (Berens, 2009) for MATLAB. The same procedures were used to determine delta–spindle PAC, using a filter of 0.75–4.25 Hz for the delta frequency band.

Slow oscillation/delta nesting index. In addition to the two above described approaches, which characterise delta-spindle interactions and SO-spindle interactions in more detail, we calculated a sleep parameter that takes both SO–spindle and delta–spindle activity into account and was found to be the most predictive for memory consolidation in rats (Kim et al., 2019). Therefore, nested spindle events were defined according to previously used criteria (amplitude: 25% highest amplitudes, duration: 0.5–3 s), with their centre occurring within −0.5 to +0.5 s around the up-state of the SO or delta wave, respectively. If a spindle occurred within the nesting window of both, a SO and a delta wave, it was allocated to the event with the smallest time difference between the slow wave up-state and the spindle centre. To determine SO nesting, all spindles nested to SOs were counted. Delta nesting was determined by counting the number of delta-nested spindles in each nap. Equivalent to the original rodent study (Kim et al., 2019), we calculated the SO/delta nesting index for each nap by dividing the number of SO-nested spindles by the number of delta-nested spindles. Nesting analyses were calculated for each nap separately. To explore associations with memory performance, averages were calculated over all nap conditions for SO–spindle and delta–spindle coupling measures, as well as for the SO/delta nesting index.

2.4.3 | Interdependence between delta activity and SO-related spindles

In light of recently published results on the interdependence between SO- and delta-related activity in rats using optogenetic stimulation (Kim et al., 2019), we further addressed this issue in natural human daytime sleep of older adults. We therefore compared SO–spindle coupling for low versus high delta power segments. According to the findings in rats, SO–spindle coupling was expected to deviate depending on delta power. To this end, we determined delta power by applying a Hilbert transformation on the delta band-pass (1–4 Hz) filtered data. Delta power was averaged over the 30-s epoch and all electrodes of the respective ROI. A within-subject median split was applied to distinguish between epochs of low and high delta power for each nap (Iacobucci et al., 2015). TFR analysis for SO events and PAC analysis for SO–spindle associations were repeated for low and high delta power intervals.

2.5 | Statistical analysis

To test for event-locked power differences in the TFRs, we applied two-tailed paired-samples *t* tests (group level statistics) to compare spindle power fluctuations in SOs versus delta waves. Correction for multiple comparisons (−1.2 s to +1.2 s, 5–20 Hz) was performed using a cluster-based permutation procedure as implemented in *FieldTrip* (Maris & Oostenveld, 2007). Given that phase is a circular metric, traditional analyses for repeated measures were not applicable. In line with previous studies, we expected maximal spindle power around the SO up-state (i.e., ∼0 °) and compared whether this was also the case for delta–spindle coupling using the V test (Berens, 2009).

Statistical analyses for linear metrics were conducted with R (R Core Team, 2020) using the packages lme4 (Bates et al., 2015), ICC (Wolak et al., 2012), R2glmm (Jaeger, 2017), and tidyverse (Wickham et al., 2019). Linear mixed-effect models (random intercept models) were computed for the dependent variables resultant vector length (coupling strength) and SO/delta nesting index. The repeated measurements (factor nap condition: T1, T2, T3) were level-1 units nested in individuals (level-2 units). Models included fixed effects for the oscillation (SO or delta wave), or delta power (low or high), respectively.

To test for intra-individual stability of relevant coupling measures across all nap conditions, intra-class correlation coefficients (ICCs) were calculated for both SO–spindle and delta–spindle coupling strengths (resultant vector lengths) and the SO/delta nesting index, previously used to test trait-specific nature of variability in sleep/wake parameters (Tucker et al., 2007; van Dongen et al., 2005). Resulting estimates indicate the stability of the inter-individual differences across the three naps and were interpreted according to benchmark published ranges: ‘slight’ (0.0–0.2), ‘fair’ (0.2–0.4), ‘moderate’ (0.4–0.6), ‘substantial’ (0.6–0.8), and ‘almost perfect’ (0.8–1.0) (Landis & Koch, 1977). Pearson's *r* correlation coefficients were then computed to test for a linear relationship between memory

performance (encoding, immediate recall) and SO–spindle coupling strength, delta–spindle coupling strength or SO/delta nesting index (each coupling measure averaged over the three nap conditions for each participant), corrected for age and gender. The *p* values have to be interpreted with caution in this exploratory study. In this study, 15 unadjusted *p* values are reported. Considering a two-sided significance level of 0.05 and a correction for multiple testing (Bonferroni correction) the adjusted significance level is $0.05/15 = 0.0033$. Therefore, only $p < 0.0033$ should be interpreted as statistically significant. Interpretation of results is mainly based on effect size measures such as correlation coefficients and partial R^2 values as well as on estimates and 95% confidence intervals (CIs).

3 | RESULTS

Participants slept on average for 81 min (mean [SD]: T1: 79.7 [15.2]; T2: 81.1 [16.2]; T3: 81.1 [13.0] min). Sleep architecture was comparable with previous reports in healthy older adults during daytime napping, with large proportion of lighter NREM sleep and only short to none N3 and REM sleep (mean [SD] time spent in wake: 6.0 [7.5], N1: 24.2 [15.4], N2: 44.8 [16.8], N3: 3.9 [6.5], R: 1.3 [4.1] min) (Baran et al., 2016; Ladenbauer et al., 2021). Number and density of detected oscillatory events are displayed in Table 1. As results for TFR and PAC analyses were similar between all nap conditions, we mainly report and depict results for T1, unless stated otherwise. As the same applies for the two ROIs, we depict results for the frontal ROI only (see Figures S1 an S2 for results from the centro-parietal ROI and T2, T3).

Given the limitations of the frequency approach in sharply distinguishing between SO and delta waves, we assessed how many events were included in both the delta and SO analyses. We found that in T1, a mean (SD) of 6.24 (4.40) events overlapped, in T2 7.38 (4.61), and in T3 6.06 (5.27). As we consider this a negligible proportion of all SO (3%–4%) and delta events (0.5%–0.6%), we did not address this issue in the following analysis. Besides, when Steriade et al. described the SO phenomenon in detail, they already proposed that the SO triggers and groups not only spindle but also delta activity, leading to occasional overlap of SO and delta waves at the cortical level during early N3 (Amzica & Steriade, 1998; Steriade, Nunez, Amzica, 1993).

3.1 | Slow oscillation–spindle coupling was stronger than delta–spindle coupling

As expected, averaged SO amplitude was higher in comparison to delta wave amplitude (Table 1). The typical phase dependency of fluctuating spindle power (12–15 Hz) during SO events were found to be similar for delta events in the TFR: spindle power was suppressed during the down-state (delta through), increased during the subsequent down-to-up phase transition, and reached a peak around the up-state of the delta wave (Mölle et al., 2002; Mölle et al., 2011) (Figure 1b). In the TFR analysis, no substantial difference was evident with regard to spindle power during SOs versus delta waves (Figure 1b bottom).

The PAC results are shown in Figures 1c and S1. The preferred phases of peak spindle power were similar, that is, spindle power maxima occurred preferentially in the late rising phase of both SO and delta events, although in SO events they occurred slightly more synchronised with the up-states than in delta waves, as indicated by a mean phase of SO closer to 0 ° (i.e., in phase synchrony; circular mean [SD] SO: −16.32 [40.66] versus delta: −25.18 [46.31] °). Similarly, the grey circular histograms in Figure 1b show that spindle activity in the SOs was more pronounced around the SO up-phase (0 °), whereas in delta events, the distribution was more dispersed across all phases.

TABLE 1 Number, density, and amplitudes of oscillatory events during N2/N3 sleep for the frontal regions of interest ROI. Mean (SD) values per nap are shown.

Oscillatory events during N2/N3 sleep	T1	T2	T3
Number of events			
SOs	175.25 (94.94)	101.39 (41.75)	152.78 (87.44)
Delta waves	1091.46 (534.76)	1147.99 (424.16)	1036.2 (475.09)
Spindles	312.54 (156.61)	171.24 (62.14)	304.07 (141.51)
SO-nested spindles	29.22 (19.92)	31.18 (19.5)	26.16 (21.91)
Delta-nested spindles	185.61 (110.72)	202.38 (101.36)	179.51 (106.78)
Events/min			
SO density	3.76 (0.63)	2.11 (0.26)	3.44 (0.75)
Delta density	23.97 (1.72)	24.11 (1.63)	23.58 (2.08)
Spindle density	6.87 (1.08)	3.65 (0.57)	7 (1)
SO-nested spindles	0.59 (0.22)	0.65 (0.25)	0.59 (0.28)
Delta-nested spindles	3.87 (1.02)	4.24 (1.24)	4.09 (1.22)
Event amplitudes, μV			
SO amplitude	49.78 (27.35)	55.00 (16.47)	51.13 (17.28)
Delta amplitude	38.13 (26.60)	36.27 (7.45)	35.78 (8.28)

Abbreviation: SO, slow oscillation.

This finding was confirmed by the V test statistics, indicating a higher maximum concentration of spindle power around the up-phase (i.e., around 0 °) in SO events ($V = 20.83$, $p < 0.001$) compared to delta events ($V = 17.67$, $p < 0.001$).

Importantly, a substantial difference between SO–spindle and delta–spindle coupling emerged for coupling strength, that is, resultant vector length. Due to the linearity of this metric, we were able to include data of all nap conditions by incorporating the factor nap condition in the model.

We found higher coupling strengths of spindles to SOs as compared to delta waves (model based estimates adjusted for age, sex, nap, and clustering of measures within subjects, $n = 33$ subjects/180 measures; mean difference 0.084, 95% CI 0.069–0.099; $p < 0.001$, partial $R^2 = 0.36$; Figure 1c).

3.2 | Slow oscillation–spindle coupling strength was lower in low compared to high delta power intervals

To test for interdependence between SO- and delta-related activity, separate TFR and PAC analyses of SO events were conducted for low and high delta power segments.

Time–frequency analysis revealed no substantial differences in spindle power between low and high delta power segments (Figures 2a and S2).

The PAC analyses addressing the SO–spindle phase relationships in these segments, revealed differences between low and high delta power segments. On the one hand, higher concentrations of spindle power maxima were found around the SO up-states for low delta power segments (across all SO events as well as for participant-averaged SO phases; see histogram and circles in Figure 2b and S2; low: $V = 22.04$, $p < 0.001$; high: $V = 20.37$, $p < 0.001$), indicating more synchronous SO–spindle coupling in low compared to high delta power intervals. This was also underlined by the mean SO phase angles of spindle power peak: SO–spindle coupling was closer to synchrony in low delta power intervals (circular mean [SD] SO phase −10.07 [38.71] °), as compared to high delta power intervals (−20.16 [40.65] °).

Interestingly, on the other hand, coupling strength analyses indicated an interrelation in the opposite direction: coupling strength for SO–spindle coupling was substantially lower in low as compared to high delta power segments in all three naps (model based estimates adjusted for age, sex, nap, and clustering of measures within subjects, $n = 33$ subjects/180 measures; mean difference: −0.057, 95% CI −0.079 to −0.036; $p < 0.001$, partial $R^2 = 0.11$; Figure 2c).

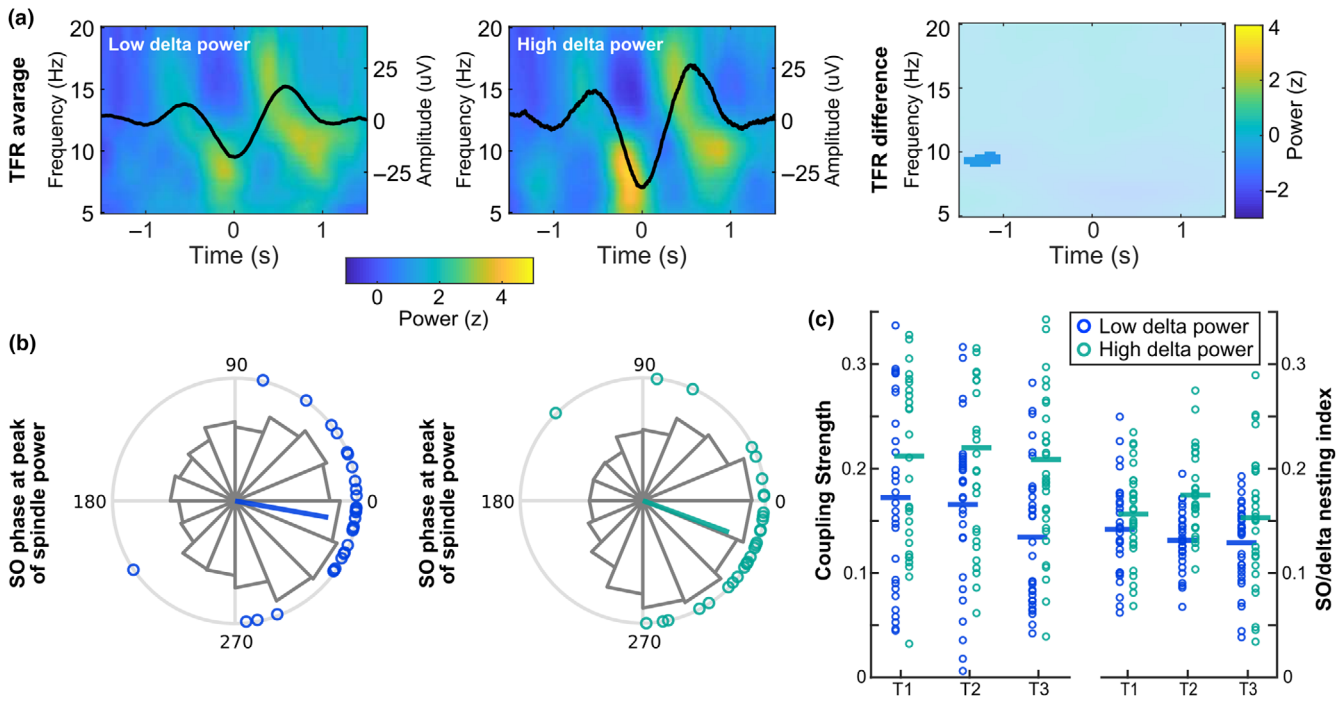

FIGURE 2 Interrelations between delta activity and slow oscillation (SO)–spindle coupling. (a) Time-frequency representations (TFRs) locked to SO and delta events of low (left, $n = 83$) and high (centre, $n = 93$) delta power intervals. Averaged power z-scores relative to pre-event baseline distributions are shown. Black lines indicate grand average SO events. Right, Difference of low–high delta power TFRs masked by significance (right, $p < 0.05$; corrected for multiple comparison). (b) SO–spindle phase–amplitude coupling for intervals of low (blue) and high (cyan) delta power, respectively. Histogram indicates distribution of SO phase angle at peak of spindle power across all SO events. Circles represent averages per participant and the coloured line denotes the corresponding resulting vector length across all participants. (c) Coupling strength and SO/delta nesting index for SO–spindle coupling per participant in intervals of low and high delta power. Bars denote means across participants for each nap condition (T1, T2, T3). SO/delta nesting index is the ratio of SO-nested spindles and delta nested spindles.

Additionally, we compared SO/delta nesting index between low and high delta power segments and found lower spindle nesting to SOs in the low compared to the high delta power condition (model based estimates adjusted for age, sex, nap, and clustering of measures within subjects, $n = 33$ subjects/180 measures; mean difference: −0.027, 95% CI −0.039 to −0.015; $p < 0.001$, partial $R^2 = 0.099$). Please see also Table 2 for numbers of nested spindles. We have furthermore compared number of SO events and their amplitudes for high versus low delta power intervals and found that SO events were more frequent in intervals with high delta power compared to low delta power intervals (please see the Supporting Information, Data S1, Table S1). Similarly, SO amplitudes were higher in high delta power intervals.

3.3 | Coupling parameters were stable over multiple naps

To further examine whether coupling strength of SO–spindle and delta–spindle coupling were stable over multiple naps within individuals, ICC values were calculated. In addition, the intra-individual stability was likewise investigated for the SO/delta nesting index. ICC estimates indicated 'moderate' stability of delta–spindle coupling strength (0.46, 95% CI 0.22–0.66), a 'fair' stability of SO–spindle coupling strength (0.29, 95% CI −0.20 to 0.24) and 'fair' stability of the SO/delta nesting index (0.31, 95% CI 0.08–0.54) according to published benchmarks (Landis & Koch, 1977). As such delta–spindle coupling, SO–spindle coupling, and the SO/delta nesting index can be considered at least fairly stable within subjects across three naps.

3.4 | Nesting index indicated strongest correlation with the ability to form novel memories

To test for possible associations with the ability to form novel memories, we have averaged the coupling strength measures as well as SO/delta nesting index over the three naps; and controlled for the effect of age and gender. We found a positive association between SO/delta nesting index and superior performance during encoding ($r = 0.35$, $p = 0.046$). In addition, a trend for a positive association between SO/delta nesting index and immediate recall was observed ($r = 0.33$, $p = 0.06$, Figure 3a). SO–spindle coupling strength (encoding: $r = 0.08$, $p = 0.66$; recall: $r = 0.28$, $p = 0.12$, Figure 3b) and delta–spindle coupling strength (encoding: $r = 0.18$, $p = 0.31$; recall: $r = 0.17$, $p = 0.34$, Figure 3c) were not associated with memory performance. Statistical testing of differences between correlations revealed no substantial differences (all $p > 0.1$) (Lenhard & Lenhard, 2014). Circular-linear correlation of SO–spindle coupling phase with memory likewise indicated only weak associations (encoding: $r = 0.10$, $p = 0.84$; recall: $r = 0.29$, $p = 0.23$).

4 | DISCUSSION

Our results revealed similarly timed but weaker delta–spindle compared to SO–spindle coupling in healthy older adults. Moreover, delta–spindle coupling varied between individuals, but was relatively stable intra-individually. We found no evidence for an inverse dependence between SO- and delta-related activities during NREM sleep, contrary to our initial hypothesis. Furthermore, the ratio of SO- and delta-nested spindles, rather than measures of SO–spindle and delta–spindle coupling in isolation, were associated with the ability to form new memories.

With regard to delta–spindle interrelations, we showed a temporal clustering of spindles in delta waves in older humans, in line with an earlier finding in adult rats (Kim et al., 2019). We have implemented an approach that allowed us to provide detailed information about phase and strength of delta–spindle coupling, and to compare spindle coupling among oscillations of diverging frequencies (e.g., SO and delta). We found similar patterns with regard to the average timing of spindle power maxima within the slow-waves phase: in both cases, peak spindle activity peaked on average during the late rising phase of the slow waves. However, coupling strength with spindles was much stronger for SOs as compared to delta waves, indicating a much stronger consistency in the preferred phase of spindle activity during SO events, which can be interpreted in line with global versus local processes (Genzel et al., 2014). It can be assumed that the high amplitude SOs were more globally synchronised across cortical and sub-cortical regions than delta waves (Bernardi et al., 2018), thereby enabling a stronger driving role on thalamic networks and on the generation as well as timed modulation of sleep spindles (Mak-McCully et al., 2017).

By exploring SO–spindle coupling and the ratio of SO-nested spindles to delta-nested spindles (SO/delta nesting index) separately in sleep periods of low and high delta power, we aimed to unveil the proposed opposing dependency between SO- and delta-related activity, which was found by disrupting spiking activity either during SOs

TABLE 2 Slow oscillation (SO)- and delta-nested spindles and the SO/delta nesting index for intervals of low and high delta power. Mean (SD) values per nap are shown.

Nap (mean number of 30-s intervals/nap)	Low delta power			High delta power		
	T1 (49)	T2 (51)	T3 (47)	T1 (49)	T2 (50)	T3 (47)
SO-nested spindles	11.7 (7.8)	13.1 (8.4)	10.3 (8.3)	16.4 (10.9)	17.5 (9.5)	14.2 (11.7)
Delta-nested spindles	83.1 (49.9)	95.7 (49.6)	78.1 (51.3)	97.3 (55.8)	100.5 (45.6)	89.3 (47.5)
SO/delta nesting index	0.14 (0.05)	0.13 (0.03)	0.13 (0.04)	0.16 (0.04)	0.18 (0.04)	0.15 (0.06)

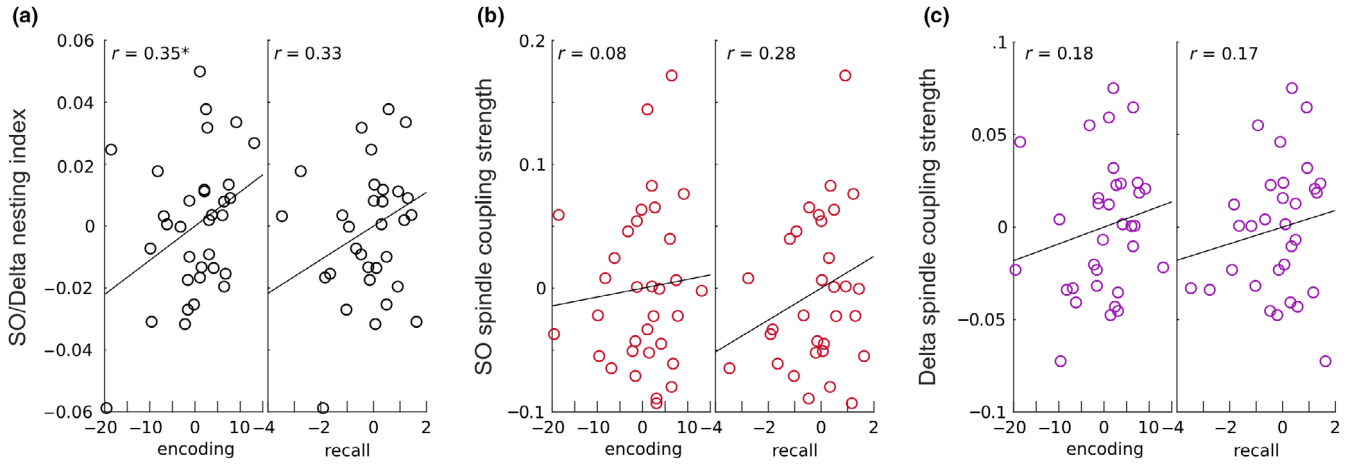

FIGURE 3 Association with memory. Scatter plots of partial correlation (after eliminating variations explained by age and gender) for the Auditory Verbal Learning Test encoding and immediate recall with SO/delta nesting index (a), SO–spindle coupling strength (b), and delta–spindle coupling strength (resultant vector length) (c). The SO/delta nesting index was positively associated with better encoding and trend wise with better immediate recall, while no correlation was found for SO–spindle and delta–spindle coupling strength with memory performance. SO/delta nesting index is the ratio of SO- and delta-nested spindles. Black lines show the trend lines. *$p < 0.05$.

or during delta waves using optogenetic stimulation in rodents (Kim et al., 2019). When delta waves were disturbed, their amplitudes were reduced, followed closely by an increase in SO–spindle nesting. Given these findings reciprocal interactions between SOs and delta waves were proposed, that may enable a competitive balance between consolidation and homeostasis during sleep. Unexpectedly and at odds with this hypothesis, we found higher coupling strength in high compared to low delta power intervals in older human participants. Surprisingly, similar to coupling strength, the SO/delta nesting index was higher in the high delta power condition. Thus, we were not able to confirm a competitive interaction between SO and delta-wave activity during natural human sleep.

The discrepancy in findings may point to a specificity of species, age, and/or may arise from differences in study design. As we were interested in the interaction between delta- and SO-related activity during natural (unperturbed) sleep in humans, time periods of differing delta power were selected and compared. Thereby, we were able to evaluate a temporal association between delta- and SO-related activity but could not probe causal interactions using a perturbation approach. As our complementary analyses revealed that SOs are more frequently present and have higher amplitudes in intervals with high delta power, this may provide a partial explanation for the present results. Further, competitive interactions between SO and delta may also be more locally restricted and therefore only become evident in local field potential recordings but not in EEG signals providing macroscale information on neural activity (Fröhlich, 2016).

In a last step, we were interested whether SO–spindle and delta–spindle coupling exhibit a trait-like character and may be of predictive value for the individual ability to form novel memories. Consistent with a previous finding (Cox et al., 2018), our results during daytime napping indicate intra-individual stability of coupling parameters, in line with the trait-like hypothesis. Of note, delta–spindle coupling strength indicated highest stability, while SO–spindle coupling strength and the SO/delta nesting index showed lower ('fair') consistency between the three nap sessions. The lower stability of these two parameters may be due to differences between nap and nocturnal sleep.

Interestingly, the SO/delta nesting index was positively associated with individual ability to form novel memories, while delta–spindle as well as SO–spindle coupling strength by themselves were not. This finding underscores the relevance of interactions between SO- and delta-spindle nesting and points towards a competitive role of SO- versus delta-nested spindles in memory formation, in which SO-nested spindles promote memory formation, while delta-nested spindles seem to impede this process or actively promote forgetting. In contrast to Kim et al. (2019), we did not investigate sleep-dependent memory consolidation, but the ability to form novel memories as a function of the participant's characteristic micro-sleep parameters. Despite this difference, our findings can be considered consistent with a framework in which SO-nested spindles—coupled to hippocampal ripples—can promote bi-directional communication between the hippocampus and neocortex during sleep, enabling the transfer of prior hippocampal-dependent representations to neocortical long-term storage sites (Klinzing et al., 2019). This transfer to a more neocortical representation simultaneously restores hippocampal encoding capacity (Walker, 2009) and may thus enhance the ability to form novel memories.

An unanswered question in Kim et al. (2019) was whether delta-related activity supported forgetting by participating in synaptic downscaling, or whether delta exerted its effects by merely attenuating consolidation effects, possibly by impacting on SO- and spindle-generating networks (Kim et al., 2019; Ngo & Born, 2019). Assuming that synaptic downscaling promotes encoding of new memories, relatively more delta-nested spindles should be favourable for memory formation. However, we found the opposite relationship, with more SO-nested spindles relative to delta-nested spindles facilitating memory formation. Thus, taken together, our behavioural results support the notion that interactions between SOs and delta waves during

sleep may drive competing processes related to memory, but do not indicate that synaptic downscaling is involved in these processes.

Several limitations should be considered when interpreting our findings: first, in accordance with the conventions for differentiating slow waves into SOs and delta waves (Klinzing et al., 2019), as well as previous findings that speak in favour of the frequency criterion (Achermann & Borbély, 1997; Mölle et al., 2002), we chose to use that as the main criterion to distinguish the waveforms. Although this choice led to a small overlap between SO and delta events, it is more appropriate for older individuals. Indeed, age differences in slow-wave frequency are relatively small and remain within the frequency range of 0.5–1 Hz, whereas slow-wave amplitudes show marked reductions with age (Muehlroth & Werkle-Bergner, 2020). In the original rodent study (Kim et al., 2019), a down-state amplitude criterion was used for differentiation between SOs and delta waves instead. Despite this difference, results still reveal similar distinction in slow-wave properties: SO and delta waves differ substantially in their amplitudes.

Second, we used the spindle frequency range 12–15 Hz that was demonstrated to play an essential role in the context of SO coupling and memory consolidation (Mölle et al., 2011). However, given previous evidence on large between-subject variability of slow and fast spindle frequency and topography (Cox et al., 2017), an individualised approach for spindle frequency assessment might also be considered in future studies.

Moreover, this study was an exploratory analysis of an existing data set that comprised nap sleep in older adults only. The additional inclusion of young subjects would lead to increased generalisability of our results. Moreover, inclusion of nocturnal sleep, which is rich in N3 (where delta waves and SOs predominate), would be favourable, even though the fraction of global slow waves was previously shown to be larger for N2 than N3 (Malerba et al., 2019).

In summary, our results show differences between delta waves and SOs in terms of amplitude and coupling strength with spindles, which may at least contribute to functional differences. Unlike recent findings in rodents, no evidence was found for opposing dependency between delta activity and SO–spindle coupling during natural sleep of healthy older human participants. However, in functional terms our data similarly suggests that SOs, delta waves and spindles should be jointly considered when aiming to link sleep physiology and memory formation. In this respect, our findings support the notion that SO–spindle coupling and delta–spindle coupling may serve distinct functional roles with regard to memory processes. Future studies in humans should investigate whether a precisely timed manipulation of slow-wave oscillations by non-invasive brain stimulation would reveal a competitive interplay between delta- and SO-related activity.

AUTHOR CONTRIBUTIONS

Larissa N. Wüst: Data curation; formal analysis; investigation; methodology; visualization; writing – original draft; writing – review and editing. **Daria Antonenko:** Validation; writing – original draft; writing – review and editing. **Robert Malinowski:** Data curation; formal analysis; methodology; supervision. **Liliia Khakimova:** Data curation; formal analysis; investigation. **Ulrike Grittner:** formal analysis (statistical analyses). **Klaus Obermayer:** Conceptualization; funding acquisition; writing – review and editing. **Julia Ladenbauer:** Conceptualization; funding acquisition; investigation; methodology; project administration; supervision; validation; visualization; writing – original draft; writing – review and editing. **Agnes Flöel:** Conceptualization; funding acquisition; investigation; supervision; validation; writing – review and editing.

ACKNOWLEDGEMENTS

This work was supported by the Deutsche Forschungsgemeinschaft (327654276 – SFB 1315 B03, to Agnes Flöel and Klaus Obermayer). We thank Daniela Obst and Eric Tönnies for help with data acquisition. Open Access funding enabled and organized by Projekt DEAL.

CONFLICT OF INTEREST STATEMENT

The authors have no conflict of interest to declare.

DATA AVAILABILITY STATEMENT

The data of this study are available from the corresponding authors upon reasonable request with a formal data sharing agreement.

ORCID

Larissa N. Wüst https://orcid.org/0000-0003-0392-1430
Julia Ladenbauer https://orcid.org/0000-0001-5060-250X

REFERENCES

Achermann, P., & Borbély, A. A. (1997). Low-frequency (<1 Hz) oscillations in the human sleep electroencephalogram. *Neuroscience*, *81*(1), 213–222. https://doi.org/10.1016/s0306-4522(97)00186-3

Amzica, F., & Steriade, M. (1998). Electrophysiological correlates of sleep delta waves. *Electroencephalography and Clinical Neurophysiology*, *107*(2), 69–83.

Aru, J., Aru, J., Priesemann, V., Wibral, M., Lana, L., Pipa, G., … Vicente, R. (2015). Untangling cross-frequency coupling in neuroscience. *Current Opinion in Neurobiology*, *31*, 51–61. https://doi.org/10.1016/j.conb.2014.08.002

Baran, B., Mantua, J., & Spencer, R. M. C. (2016). Age-related changes in the sleep-dependent reorganization of declarative memories. *Journal of Cognitive Neuroscience*, *28*(6), 792–802. https://doi.org/10.1162/jocn_a_00938

Bates, D., Mächler, M., Bolker, B., & Walker, S. (2015). Fitting linear mixed-effects models using lme4. *Journal of Statistical Software*, *67*(1), 1–48. https://doi.org/10.18637/jss.v067.i01

Berens, P. (2009). CircStat: A MATLAB toolbox for circular statistics. *Journal of Statistical Software*, *31*(10), 21. https://doi.org/10.18637/jss.v031.i10

Bernardi, G., Siclari, F., Handjaras, G., Riedner, B. A., & Tononi, G. (2018). Local and widespread slow waves in stable NREM sleep: Evidence for distinct regulation mechanisms. *Frontiers in Human Neuroscience*, *12*, 248. https://doi.org/10.3389/fnhum.2018.00248

Cox, R., Mylonas, D. S., Manoach, D. S., & Stickgold, R. (2018). Large-scale structure and individual fingerprints of locally coupled sleep oscillations. *Sleep*, *41*(12), 1–15. https://doi.org/10.1093/sleep/zsy175

Cox, R., Schapiro, A. C., Manoach, D. S., & Stickgold, R. (2017). Individual differences in frequency and topography of slow and fast sleep spindles. *Frontiers in Human Neuroscience*, *11*, 1–22. https://doi.org/10.3389/fnhum.2017.00433

Fröhlich, F. (2016). Chapter 10 - LFP and EEG. In F. Fröhlich (Ed.), *Network neuroscience* (pp. 127–143). Academic Press. https://doi.org/10.1016/B978-0-12-801560-5.00010-0

Genzel, L., Kroes, M. C. W., Dresler, M., & Battaglia, F. P. (2014). Light sleep versus slow wave sleep in memory consolidation: A question of global versus local processes? *Trends in Neurosciences*, *37*(1), 10–19. https://doi.org/10.1016/j.tins.2013.10.002

Göder, R., Baier, P. C., Beith, B., Baecker, C., Seeck-Hirschner, M., Junghanns, K., & Marshall, L. (2013). Effects of transcranial direct current stimulation during sleep on memory performance in patients with schizophrenia. *Schizophr Res*, *144*(1–3), 153–154. https://doi.org/10.1016/j.schres.2012.12.014

Helfrich, R. F., Mander, B. A., Jagust, W. J., Knight, R. T., & Walker, M. P. (2018). Old brains come uncoupled in sleep: Slow wave-spindle synchrony, brain atrophy, and forgetting. *Neuron*, *97*(1), 221–230. https://doi.org/10.1016/j.neuron.2017.11.020

Helmstaedter, C., Lendt, M., & Lux, S. (2001). *Verbaler Lern- und Merkfähigkeitstest (VLMT)*. Beltz.

Iacobucci, D., Posavac, S. S., Kardes, F. R., Schneider, M. J., & Popovich, D. L. (2015). The median split: Robust, refined, and revived. *Journal of Consumer Psychology*, *25*(4), 690–704. https://doi.org/10.1016/j.jcps.2015.06.014

Jaeger, B. (2017). r2glmm: Computes R squared for mixed (multilevel) models. *R Package Version 0.1*, *2*, 1–12.

Kim, J., Gulati, T., & Ganguly, K. (2019). Competing roles of slow oscillations and Delta waves in memory consolidation versus forgetting. *Cell*, *179*(2), 514–526. https://doi.org/10.1016/j.cell.2019.08.040

Klinzing, J. G., Niethard, N., & Born, J. (2019). Mechanisms of systems memory consolidation during sleep. *Nature Neuroscience*, *22*(10), 1598–1610. https://doi.org/10.1038/s41593-019-0467-3

Ladenbauer, J., Khakimova, L., Malinowski, R., Obst, D., Tönnies, E., Antonenko, D., … Flöel, A. (2022). Towards optimization of oscillatory stimulation during sleep. *Neuromodulation*, 1–10. https://doi.org/10.1016/j.neurom.2022.05.006

Ladenbauer, J., Kulzow, N., Passmann, S., Antonenko, D., Grittner, U., Tamm, S., & Floel, A. (2016). Brain stimulation during an afternoon nap boosts slow oscillatory activity and memory consolidation in older adults. *Neuroimage*, *142*, 311–323. https://doi.org/10.1016/j.neuroimage.2016.06.057

Ladenbauer, J., Ladenbauer, J., Kulzow, N., de Boor, R., Avramova, E., Grittner, U., & Floel, A. (2017). Promoting sleep oscillations and their functional coupling by transcranial stimulation enhances memory consolidation in mild cognitive impairment. *The Journal of Neuroscience*, *37*(30), 7111–7124. https://doi.org/10.1523/JNEUROSCI.0260-17.2017

Ladenbauer, J., Ladenbauer, J., Kulzow, N., & Floel, A. (2021). Memory-relevant nap sleep physiology in healthy and pathological aging. *Sleep*, *44*, 1–13. https://doi.org/10.1093/sleep/zsab002

Landis, J. R., & Koch, G. G. (1977). The measurement of observer agreement for categorical data. *Biometrics*, *33*(1), 159–174.

Lenhard, W., & Lenhard, A. (2014). *Hypothesis tests for comparing correlations*. *Psychometrica*.

Mak-McCully, R. A., Rolland, M., Sargsyan, A., Gonzalez, C., Magnin, M., Chauvel, P., … Halgren, E. (2017). Coordination of cortical and thalamic activity during non-REM sleep in humans. *Nature Communications*, *8*(15), 499. https://doi.org/10.1038/ncomms15499

Malerba, P., Whitehurst, L. N., Simons, S. B., & Mednick, S. C. (2019). Spatio-temporal structure of sleep slow oscillations on the electrode manifold and its relation to spindles. *Sleep*, *42*(1), zsy197.

Maris, E., & Oostenveld, R. (2007). Nonparametric statistical testing of EEG- and MEG-data. *Journal of Neuroscience Methods*, *164*(1), 177–190. https://doi.org/10.1016/j.jneumeth.2007.03.024

Mikutta, C., Feige, B., Maier, J. G., Hertenstein, E., Holz, J., Riemann, D., & Nissen, C. (2019). Phase-amplitude coupling of sleep slow oscillatory and spindle activity correlates with overnight memory consolidation. *Journal of Sleep Research*, *28*(6), e12835. https://doi.org/10.1111/jsr.12835

Mölle, M., Bergmann, T. O., Marshall, L., & Born, J. (2011). Fast and slow spindles during the sleep slow oscillation: Disparate coalescence and engagement in memory processing. *Sleep*, *34*(10), 1411–1421. https://doi.org/10.5665/sleep.1290

Mölle, M., Eschenko, O., Gais, S., Sara, S. J., & Born, J. (2009). The influence of learning on sleep slow oscillations and associated spindles and ripples in humans and rats. *European Journal of Neuroscience*, *29*(5), 1071–1081. https://doi.org/10.1111/j.1460-9568.2009.06654.x

Mölle, M., Marshall, L., Gais, S., & Born, J. (2002). Grouping of spindle activity during slow oscillations in human non-rapid eye movement sleep. *The Journal of Neuroscience*, *22*(24), 10941–10947. https://doi.org/10.1523/jneurosci.22-24-10941.2002

Muehlroth, B. E., & Werkle-Bergner, M. (2020). Understanding the interplay of sleep and aging: Methodological challenges. *Psychophysiology*, *57*(3), e13523. https://doi.org/10.1111/psyp.13523

Ngo, H. V., & Born, J. (2019). Sleep and the balance between memory and forgetting. *Cell*, *179*(2), 289–291. https://doi.org/10.1016/j.cell.2019.09.007

Oostenveld, R., Fries, P., Maris, E., & Schoffelen, J. M. (2011). FieldTrip: Open source software for advanced analysis of MEG, EEG, and invasive electrophysiological data. *Computational Intelligence and Neuroscience*, *2011*(156), 869. https://doi.org/10.1155/2011/156869

Rasch, B., & Born, J. (2013). About sleep's role in memory. *Physiological Reviews*, *93*(2), 681–766. https://doi.org/10.1152/physrev.00032.2012

Rechtschaffen, A., & Kales, A. (1968). Techniques and scoring system for sleep stages of human subjects. *A Manual of Standardized Terminology* https://ci.nii.ac.jp/naid/10008107654/en/

Staresina, B. P., Bergmann, T. O., Bonnefond, M., van der Meij, R., Jensen, O., Deuker, L., … Fell, J. (2015). Hierarchical nesting of slow oscillations, spindles and ripples in the human hippocampus during sleep. *Nature Neuroscience*, *18*(11), 1679–1686. https://doi.org/10.1038/nn.4119

Steriade, M., McCormick, D. A., & Sejnowski, T. J. (1993). Thalamocortical oscillations in the sleeping and aroused brain. *Science*, *262*(5134), 679–685. https://doi.org/10.1126/science.8235588

Steriade, M., Nunez, A., & Amzica, F. (1993). Intracellular analysis of relations between the slow (< 1 Hz) neocortical oscillation and other sleep rhythms of the electroencephalogram. *The Journal of Neuroscience*, *13*(8), 3266–3283. https://doi.org/10.1523/JNEUROSCI.13-08-03266.1993

Tucker, A. M., Dinges, D. F., & Van Dongen, H. P. (2007). Trait interindividual differences in the sleep physiology of healthy young adults. *Journal of Sleep Research*, *16*(2), 170–180. https://doi.org/10.1111/j.1365-2869.2007.00594.x

van Dongen, H. P. A., Vitellaro, K. M., & Dinges, D. F. (2005). Individual differences in adult human sleep and wakefulness: Leitmotif for a research agenda. *Sleep*, *28*(4), 479–498. https://doi.org/10.1093/sleep/28.4.479

Walker, M. P. (2009). The role of sleep in cognition and emotion. *Annals of the New York Academy of Sciences*, *1156*, 168–197. https://doi.org/10.1111/j.1749-6632.2009.04416.x

Wickham, H., Averick, M., Bryan, J., Chang, W., McGowan, L. D. A., François, R., … Hester, J. (2019). Welcome to the Tidyverse. *Journal of Open Source Software*, *4*(43), 1686.

Wolak, M. E., Fairbairn, D. J., & Paulsen, Y. R. (2012). Guidelines for estimating repeatability. *Methods in Ecology and Evolution*, *3*(1), 129–137. https://doi.org/10.1111/j.2041-210X.2011.00125.x

SUPPORTING INFORMATION

Additional supporting information can be found online in the Supporting Information section at the end of this article.

How to cite this article: Wüst, L. N., Antonenko, D., Malinowski, R., Khakimova, L., Grittner, U., Obermayer, K., Ladenbauer, J., & Flöel, A. (2024). Interrelations and functional roles of key oscillatory activities during daytime sleep in older adults. *Journal of Sleep Research*, *33*(3), e13981. https://doi.org/10.1111/jsr.13981